Adapting Gas Fermenting Bacteria for Light-driven Domino Valorization of CO_2

Lin Su[1, ‡], Santiago Rodríguez-Jiménez[1, ‡], Marion I. M. Short[1], Erwin Reisner[1, *]

[1] Yusuf Hamied Department of Chemistry, University of Cambridge, Cambridge, U.K.

Corresponding Author

Erwin Reisner. Email: reisner@ch.cam.ac.uk

Author Contributions

‡Lin Su and Santiago Rodríguez-Jiménez contributed equally.

ABSTRACT: We report the adaptive laboratory evolution (ALE) of *Clostridium ljungdahlii* (*Cl*) for enhanced syngas fermentation, enabling its integration into a photocatalytic CO_2-to-syngas conversion system for the upcycling of CO_2 to C_2 products, acetate and ethanol. The adapted strain, Cl_{adapt}, exhibits a 2.5-fold increase in growth rate and a 120-fold enhancement in C_2 production compared to the wild-type (Cl_{wt}). Isotopic labeling confirmed Cl_{adapt}'s high conversion efficiency, yielding 6:1 and 9:1 ratios of ^{13}C:^{12}C in acetate and ethanol, respectively. Whole genome sequencing revealed eight unique mutations in Cl_{adapt}, whereas RNA-seq identified significant alterations in gene expression, shedding light on its enhanced metabolism. Coupling Cl_{adapt} with a CO_2-to-syngas converting semiconductor-molecule hybrid photocatalyst, TiO_2|phosphonated Co(terpyridine)$_2$, enabled the assembly of a photocatalytic domino system for $CO_2 \rightarrow$syngas$\rightarrow C_2$ conversion. This study offers a streamlined approach to improving syngas fermentation in *Cl*, insights into microbial adaptability, and an ALE-guided pathway for solar-powered CO_2 upcycling using an inorganic-bacterial cascade strategy.

KEYWORDS: *Clostridium ljungdahlii, gas fermentation, adaptive laboratory evolution, semi-artificial photosynthesis*

INTRODUCTION

Semi-artificial photosynthesis merges synthetic and biological approaches to produce sustainable fuels using sunlight, particularly excelling in selective multicarbon product formation via biocatalysis.[1,2] A hybrid solar water splitting–biosynthetic system has been reported, where intermediate green H_2 is used as a reductant to fix CO_2 and efficiently produce biomass and fuels using *Cupriavidus necator*.[3] Coupling a synthetic photocatalyst with *Shewanella oneidensis* resulted in selective hydrogenation of C=C and C=O bonds.[4] The photosensitization of *Moorella thermoacetica* with extracellular CdS or intracellular gold nanoclusters established a novel pathway for photocatalytic CO_2 utilization, integrating microbial systems with nanomaterials to enhance photosynthetic efficiency.[5,6]

Gas fermenting acetogenic bacteria, particularly *Clostridium* species, have emerged as versatile platforms for producing biofuels and biochemicals from syngas, a mixture of H_2, CO and CO_2.[7–9] These *Clostridium* strains utilize the Wood-Ljungdahl pathway, which consists of two branches (**Figure 1A**) to produce the C_2 compounds: the methyl branch, reducing CO_2 to formate and further to a methyl group, and the carbonyl branch, which forms an acetyl group from CO. *Clostridium ljungdahlii* (*Cl*) has shown promise in fermenting these gases into valuable products, underscoring the economic viability of this approach in biotechnology. For instance, a carbon-negative fermentation process using engineered and closely related *Clostridium autoethanogenum* to convert waste gas feedstocks into acetone and isopropanol with high efficiency.[10] A Ag-catalyst based gas diffusion electrolyzer for CO_2-to-syngas conversion was coupled with syngas-fermenting *C. autoethanogenum* and *C. kluyveri*, producing butanol and hexanol with high selectivity and therefore offers a sustainable pathway for industrial chemical production from CO_2 and water using renewable energy.[11]

To further harness and optimize the metabolic capabilities of these microorganisms, adaptive laboratory evolution (ALE) emerges as a powerful tool to select and enhance beneficial traits without the need for genetic engineering. The principles and applications of ALE have demonstrated its simplicity and efficacy in tailoring microbial phenotypes for improved industrial performance.[12,13] Examples of successful ALE applications illustrate the transferability, flexibility and transformative potential of ALE in metabolic engineering and synthetic biology.[14–19] For example, ALE of *Sporomusa ovata* integrated with light-harvesting silicon nanowires led to a 2.4-fold increase in CO_2-reducing current density, enhancing bioelectrochemical CO_2 reduction.[16] Similarly, *C. autoethanogenum* strains developed through ALE showed superior growth and product profiles in continuous bioreactor cultures.[19] ALE using CO_2 and H_2, with other *C. autoethanogenum* lineages exposed to 2% CO, has also significantly enhanced growth rates and

ethanol production, revealing extensive proteome and metabolome changes that highlight new targets for metabolic engineering.[20]

Here, we explore for the first time the synergistic potential of ALE-derived gas-fermenting bacteria and photocatalysis for the overall conversion of CO_2 to acetate and ethanol (**Figure 1A**). A new strain of *Clostridium ljungdahlii* has been adapted for improved syngas-to-acetate conversion, which is subsequently coupled to a synthetic CO_2-to-syngas photocatalyst to demonstrate an overall CO_2→syngas→acetate domino-reaction. We therefore present a novel and alternative strategy for solar energy conversion to multicarbon chemicals and biomass that harnesses the symbiotic strength of synthetic and biological catalyst.

RESULTS AND DISCUSSION

For ALE of the commercial *C. ljungdahlii* wild-type strain (DSMZ 13528), it was first inoculated in PETC medium (ATCC Medium 1754) containing 5.0 g L^{-1} fructose (**Figure 1B**). The resulting culture was preserved with 20% glycerol at –80 °C, designated as Cl_{wt}. Subsequent transfers (trans1 to trans9, **Figures 1B and S1**) involved gradually reducing the fructose concentration while maintaining the syngas concentration constant (25% CO, 10% H_2, 65% CO_2, 112 mL headspace) as carbon and energy sources. Then, the culture was grown exclusively on syngas over 11 transfers, with fructose removed entirely. Each transfer in both stages lasted 72 hours, with incubation at 37 °C and 150 rpm. The final adapted culture (trans20) was preserved similarly, and designated as Cl_{adapt} (**Figure 1B**). We monitored OD_{600} at the start and end of each transfer (**Figure S2**), confirming consistent growth throughout the adaptation process.

To validate the success of ALE, we assessed bacterial growth on syngas under batch and continuous flow conditions (**Figure S3**), simulating potential future application designs.[21] Cell populations were monitored via OD_{600} readings, and C_2 products (acetate and ethanol) were quantified using quantitative ^{1}H NMR (qNMR) spectroscopy (**Figure 1C, 1D**). The adapted strain, Cl_{adapt}, exhibited faster growth and higher final OD_{600} values than the wildtype Cl_{wt} in both modes. In batch mode, Cl_{adapt} reached an OD_{600} increase (ΔOD_{600}) of 0.043 ± 0.002 by day 4, approximately 2.5 times higher than the 0.017 ± 0.003 ΔOD_{600} of Cl_{wt} (**Figure S4**). In continuous flow mode, by day 6, Cl_{adapt} and Cl_{wt} recorded OD_{600} values of 1.021 ± 0.343 and 0.091 ± 0.117, respectively, indicating an 11.2-fold increase in the adapted strain. Growth rate analysis (**Table S1**) showed that Cl_{adapt} had rates of 0.376 ± 0.022 per day in batch mode and 0.959 ± 0.106 per day in flow mode, compared to Cl_{wt}'s slower rates of 0.255 ± 0.007 and 0.232 ± 0.215 per day, respectively (**Figure S5**). The enhanced growth of Cl_{adapt} under flow mode suggests

improved syngas utilization following ALE, likely due to increased CO tolerance, as previous studies have shown high CO concentrations can impede growth rates.[22,23]

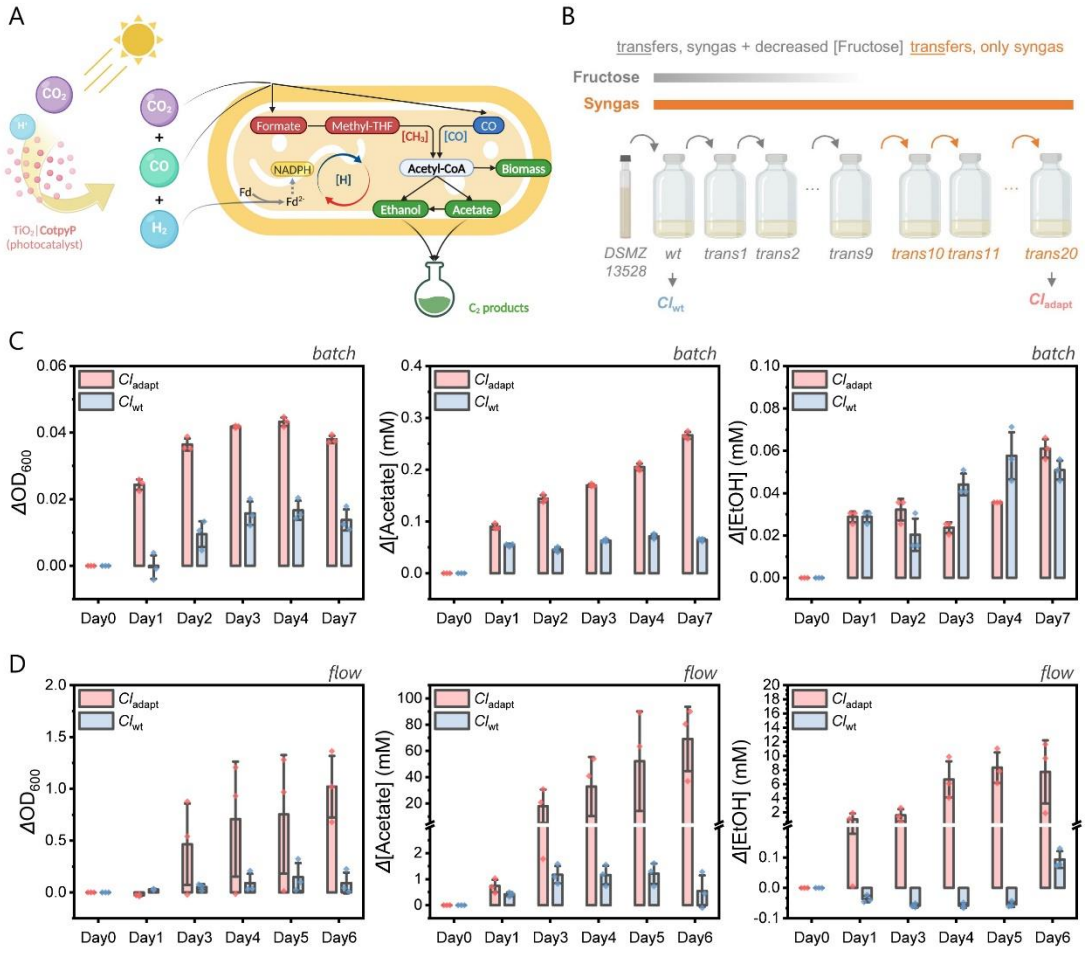

Figure 1. ALE of *Clostridium ljungdahlii*. (A) Schematic illustration of the syngas-fermenting metabolic pathways in *C. ljungdahlii*, including integration with photocatalytic syngas production. [CH_3] (red color), methyl branch; [CO] (blue color), carbonyl branch. (B) Schematic summary of the ALE process. The wild-type strain (Cl_{wt}) was adapted to a syngas environment through gradual fructose reduction and removal over 20 transfers, resulting in the adapted strain (Cl_{adapt}). (C) Comparative analysis of growth and C_2 product generation (acetate and ethanol) between Cl_{adapt} and Cl_{wt} under batch gas purging conditions (syngas purging for 30 min daily, 112 mL headspace). *(D)* Similar comparative analysis under continuous gas flow conditions (10 mL syngas per min). Growth conditions: PETC medium (pH 5.9), 37 °C with 150 rpm mixing.

In batch mode (**Figure 1C**), Cl_{adapt} produced 0.27 ± 0.01 mM acetate and 0.061 ± 0.005 mM ethanol over seven days, amounting to 0.047 ± 0.02 mM C_2 compounds per day from syngas. In contrast, Cl_{wt} produced 0.064 ± 0.003 mM acetate and 0.051 ± 0.005 mM ethanol, equivalent to 0.016 ± 0.001 mM C_2 compounds per day, approximately

three-fold less than *Cl*adapt, consistent with the observed growth rate differences. Under continuous flow mode (**Figure 1D**), *Cl*adapt generated 69.1 ± 28.3 mM acetate and 7.7 ± 5.2 mM ethanol in six days, translating to 12.8 ± 5.6 mM C_2 compounds per day. In contrast, *Cl*wt generated 0.54 ± 0.70 mM acetate and 0.09 ± 0.03 mM ethanol, or 0.11 ± 0.12 mM C_2 compounds per day, approximately 120-fold lower than *Cl*adapt. This large discrepancy suggests that continuous flow conditions, providing sustained syngas availability, greatly enhance the performance of *Cl*adapt. These findings confirm the successful adaptation of *Cl*adapt to syngas, demonstrating significantly higher C_2 compound production, especially under continuous flow operation.

To confirm the source of carbon in the C_2 products (**Figure 1A**), we performed isotopic labelling experiments using ^{13}C-syngas as the sole substrate for *Cl*adapt and *Cl*wt over 12 days. The isotopologues were analyzed by qNMR spectroscopy (**Figure 2A** for acetate and **Figure S6** for ethanol). *Cl*adapt and *Cl*wt showed acetate (38.2 and 5.3 mM) containing mixtures of ^{13}C and ^{12}C, including $^{13}CH_3$-$^{13}COO^-$, $^{13}CH_3$-$^{12}COO^-$, $^{12}CH_3$-$^{13}COO^-$, and $^{12}CH_3$-$^{12}COO^-$. However, only *Cl*adapt produced ethanol (0.7 mM) containing mixtures of $^{13}CH_3$-$^{13}CH_2OH$ and $^{12}CH_3$-$^{13}CH_2OH$. For further discussion, see **Supplementary Note 1**. The ^{13}C/^{12}C ratios were 86:14 for acetate and 95:5 for ethanol in *Cl*adapt, and 70:30 for acetate in *Cl*wt, indicating that the majority of carbon in the products originates from ^{13}C-syngas, with a smaller portion of ^{12}C likely coming from the parental culture or cellular carbon reserves. This finding confirms that both *Cl*adapt and *Cl*wt can produce C_2 compounds by converting the carbon in syngas. The higher ^{13}C content and the presence of ethanol as a more reduced product in *Cl*adapt indicates better syngas uptake and conversion activity compared to *Cl*wt[24]

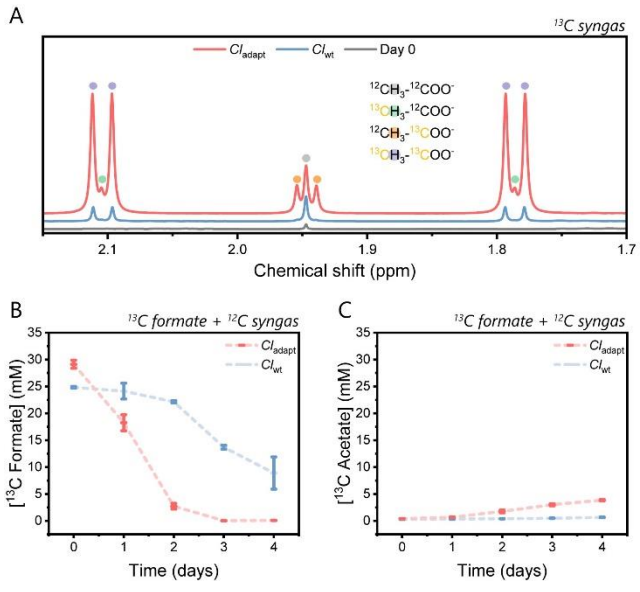

Figure 2. Growth Analysis of Strains Using ^{13}C- and ^{13}C/^{12}C Mixed-Substrates. (A) qNMR spectra showing acetate production by *Cl*adapt and *Cl*wt, when cultivated on ^{13}C-syngas (112 mL headspace) over 12 days. (B) Consumption of ^{13}C-formate, and (C)

production of ^{13}C-acetate, when cultivated on ^{13}C-formate (~30 mM) alongside ^{12}C-syngas (112 mL headspace) over 4 days. Growth conditions: PETC medium (pH 5.9), 37 °C with 150 rpm mixing.

Notably, both strains produced less $^{13}CH_3$-$^{12}COO^-$ than $^{12}CH_3$-$^{13}COO^-$ (**Table S3**), a metabolic preference that extended to $^{12}CH_3$-$^{13}CH_2OH$ (**Table S5**). This suggests a preference for retaining the ^{12}C-methyl rather than ^{12}C-carbonyl group. Compared to *Cl*$_{wt}$ ($^{13}CH_3$-$^{12}COO^-$/$^{12}CH_3$-$^{13}COO^-$ = 0.9), the *Cl*$_{adapt}$ ($^{13}CH_3$-$^{12}COO^-$/$^{12}CH_3$-$^{13}COO^-$ = 0.5) shows a more unbalanced ^{12}C/^{13}C distribution. This observation may reflect a bottleneck in the *Cl*'s Wood-Ljungdahl pathway's methyl branch,[25] which *Cl*$_{adapt}$ has not yet overcome, or alternatively the carbonyl branch has been significantly enhanced during adaptation.

To investigate differences in the methyl branch of the Wood-Ljungdahl pathway between *Cl*$_{adapt}$ and *Cl*$_{wt}$, we performed a second isotopic labeling experiment using ^{13}C-formate and ^{12}C-syngas. *Cl*$_{adapt}$ exhibited significantly faster growth, achieving a cell population five times greater than *Cl*$_{wt}$ within four days (**Figure S8A**). *Cl*$_{adapt}$ consumed ~25 mM of ^{13}C-formate within two days, whereas *Cl*$_{wt}$ utilized only ~15 mM over four days (**Figure 2B**), resulting in a markedly higher production of ^{13}C-acetate in *Cl*$_{adapt}$ (3.86 ± 0.11 mM vs. 0.66 ± 0.06 mM) (**Figure 2C**). This finding highlights *Cl*$_{adapt}$'s enhanced efficiency in utilizing formate for such as growth and acetate production, reflecting optimized pathway dynamics compared to *Cl*$_{wt}$. For further discussion, see **Supplementary Note 2**.

We conducted whole genome sequencing and RNA-seq analysis to investigate the genetic and transcriptional changes in *Cl*$_{adapt}$ compared to *Cl*$_{wt}$. The analysis revealed specific mutations (**Table S6-S8, Figure S10**) and significant differences in gene expression (**Figure S11-S14**), particularly in pathways linked to glycine reductase and carbon-oxygen lyase activities. For a detailed account of the mutations and transcriptional profiles, please refer to **Supplementary Note 3**.

Finally, we coupled *Cl*$_{adapt}$ with syngas produced from a synthetic photocatalytic CO_2 reduction system, creating an inorganic-bacterial system capable of domino valorization of CO_2 into acetate and biomass with solar energy (**Figure 3A**). The photocatalytic system was composed of light-absorbing TiO_2 nanoparticles (P25, 365 mg) and a phosphonated cobalt(II)(terpyridine)$_2$ CO_2 reduction molecular catalyst (**CotpyP**, 20 µmol g_{TiO2}^{-1}).[26,27] During photocatalysis, the hybrid TiO_2|**CotpyP** photocatalyst was suspended in an aqueous solution (217 mL) containing 0.1 M triethanolamine (TEOA) as sacrificial electron donor and irradiated with UV-containing LED simulated sunlight (AM1.5G). CO_2 flowed over six days (flow mode), mimicking the flow conditions described above, and the photogenerated syngas was continuously flown from the photoreactor to the bioreactor (**Figure 3A**). See **Supplementary Note 4** for batch mode experiment details.

In flow mode, TiO_2|**CotpyP** produced syngas under irradiation and exhibited activities of 147.8 ± 96.8 nmol CO g_{TiO2}^{-1} min^{-1} and 367.1 ± 605.9 nmol H_2 g_{TiO2}^{-1} min^{-1} (**Table S9**). The generated solar syngas had thus a CO:H_2 ratio of ~30:70. The activity of TiO_2|**CotpyP** over time under flow conditions is significantly higher than other state-of-the-art photocatalytic flow systems (**Table S10**), and therefore well suited for our biological-inorganic assembly.

The bacterial cultures were able to increase their biomass from the start of the flow experiment until day 4, reaching a ΔOD_{600} of 0.30 ± 0.09 which remained approximately constant until day 6 (**Figure 3B**). In comparison to the batch mode, the flow configuration showed an increase in acetate from day 0 to day 6 with a maximum Δ[acetate] of 0.46 ± 0.07 mM (**Figure S15**). The lack of ethanol, lower ΔOD_{600} and Δ[acetate] can be attributed to the syngas concentration in the photocatalysis gas stream (<0.1%) as well as its formation rate by TiO_2|**CotpyP** compared to the utilized commercial syngas cylinder. As shown in **Figure 1D**, Cl_{adapt} can produce high biomass and C_2 product outputs under syngas flow rates as high as 102 µmol CO min^{-1} and 41 µmol H_2 min^{-1}, highlighting the limitations of the presented photocatalytic system and need to develop improved systems capable of delivering higher syngas formation rates to Cl_{adapt}.

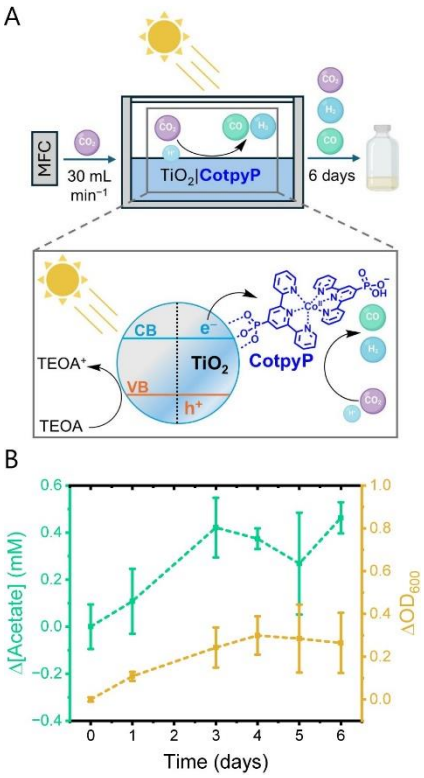

Figure 3. Light-Driven CO_2 Domino Valorization System. (A) Scheme of flow mode setup: the mass flow controller (MFC) flows CO_2 inside the photoreactor, where TiO_2|**CotpyP** generates photocatalytically syngas from 0.1M TEOA in CO_2-saturated water. An UV-containing LED simulated sunlight (AM1.5G) source irradiates the photoreactor from the top; and the bioreactor where bacteria is

cultured, receives the syngas output. (B) Variation of acetate concentration and optical density (OD_{600}) over 6 days under solar light.

Our results show that simple photocatalytic powder systems can in principle be used to feed solar syngas to gas-fermenting bacteria, thereby providing an alternative to wired devices such as electrolyzers and photoelectrochemical cells[3,5,6,11]. They also serve as a cautionary tale for researchers working in the fields of biohybrids and domino catalysis, emphasizing the need for new renewable energy-driven syngas forming systems and device architectures to fully exploit the capabilities of gas fermenting adapted bacteria, enabling high levels of C_2 products and cell growth over time.

CONCLUSION

In conclusion, our proof-of-concept approach combines for the first time photocatalytic CO_2 reduction with biosynthesis with adapted bacteria and thereby provides a blueprint for solar bioproduction of multicarbon products. It highlights the potential of enhancing microorganisms' natural abilities through adaptive evolution and their integration with inorganic catalytic systems. Future efforts will aim to optimize these biological-inorganic hybrid systems by assessing their syngas formation rates, scalability, and advancing genetic and metabolic engineering strategies to fully leverage microbial gas fermentation. This study exemplifies the transformative potential of cross-pollinating biological, materials science and chemistry innovations to tackle pressing global environmental challenges.

SUPPORTING INFORMATION

Supporting Information is available online. Including experimental details, adaptation evolution laboratory data, NMR spectra, growth calculation rates, isotopic distribution information of acetate and ethanol, genomic analysis and RNA-seq analysis of adapted and wild-type *Clostridium ljungdahlii* strains, and photocatalysis data.

COMPETING INTERESTS

The authors declare no conflict of interest.

ACKNOWLEDGMENT

This work was supported by UK Research and Innovation (European Research Council Advanced Grant, EP/X030563/1 to E.R.), a Leverhulme Trust Early Career Fellowship (ECF-2022-392 to L.S.), the Isaac Newton Trust (22.08(c) to L.S.), a European Commission Marie Sklodowska-Curie Individual Fellowship (GAN 891338 to S.R.J.), and the Engineering and Physical Sciences Research Council (EPSRC) for a NanoDTC PhD scholarship (EP/L015978/1 to M.I.M.S.). The authors thank Mr. Dongseok Kim and Dr. Leonardo Castañeda-Losada at the

University of Cambridge for helpful discussions. The authors also thank Nigel Howard at the University of Cambridge for performing elemental analyses.

REFERENCES

(1) Fang, X.; Kalathil, S.; Reisner, E. Semi-Biological Approaches to Solar-to-Chemical Conversion. *Chem. Soc. Rev.* **2020**, *49* (14), 4926–4952. https://doi.org/10.1039/c9cs00496c.

(2) Kornienko, N.; Zhang, J. Z.; Sakimoto, K. K.; Yang, P.; Reisner, E. Interfacing Nature's Catalytic Machinery with Synthetic Materials for Semi-Artificial Photosynthesis. *Nat. Nanotechnol.* **2018**, *13* (10), 890–899. https://doi.org/10.1038/s41565-018-0251-7.

(3) Liu, C.; Colón, B. C.; Ziesack, M.; Silver, P. A.; Nocera, D. G. Water Splitting–Biosynthetic System with CO2 Reduction Efficiencies Exceeding Photosynthesis. *Science* **2016**, *352* (6290), 1210–1213. https://doi.org/10.1126/science.aaf5039.

(4) Rowe, S. F.; Gall, G. L.; Ainsworth, E. V.; Davies, J. A.; Lockwood, C. W. J.; Shi, L.; Elliston, A.; Roberts, I. N.; Waldron, K. W.; Richardson, D. J.; Clarke, T. A.; Jeuken, L. J. C.; Reisner, E.; Butt, J. N. Light-Driven H2 Evolution and C C or C O Bond Hydrogenation by Shewanella Oneidensis: A Versatile Strategy for Photocatalysis by Nonphotosynthetic Microorganisms. *ACS Catal.* **2017**, *7* (11), 7558–7566. https://doi.org/10.1021/acscatal.7b02736.

(5) Zhang, H.; Liu, H.; Tian, Z.; Lu, D.; Yu, Y.; Cestellos-Blanco, S.; Sakimoto, K. K.; Yang, P. Bacteria Photosensitized by Intracellular Gold Nanoclusters for Solar Fuel Production. *Nat. Nanotechnol.* **2018**, *13* (10), 900–905. https://doi.org/10.1038/s41565-018-0267-z.

(6) Sakimoto, K. K.; Wong, A. B.; Yang, P. Self-Photosensitization of Nonphotosynthetic Bacteria for Solar-to-Chemical Production. *Science* **2016**, *351* (6268), 74–77. https://doi.org/10.1126/science.aad3317.

(7) Köpke, M.; Held, C.; Hujer, S.; Liesegang, H.; Wiezer, A.; Wollherr, A.; Ehrenreich, A.; Liebl, W.; Gottschalk, G.; Dürre, P. Clostridium Ljungdahlii Represents a Microbial Production Platform Based on Syngas. *Proc. Natl. Acad. Sci.* **2010**, *107* (29), 13087–13092. https://doi.org/10.1073/pnas.1004716107.

(8) Zhang, L.; Zhao, R.; Jia, D.; Jiang, W.; Gu, Y. Engineering Clostridium Ljungdahlii as the Gas-Fermenting Cell Factory for the Production of Biofuels and Biochemicals. *Curr. Opin. Chem. Biol.* **2020**, *59*, 54–61. https://doi.org/10.1016/j.cbpa.2020.04.010.

(9) Schulz, S.; Molitor, B.; Angenent, L. T. Acetate Augmentation Boosts the Ethanol Production Rate and Specificity by Clostridium Ljungdahlii during Gas Fermentation with Pure Carbon Monoxide. *Bioresour. Technol.* **2023**, *369*, 128387. https://doi.org/10.1016/j.biortech.2022.128387.

(10) Liew, F. E.; Nogle, R.; Abdalla, T.; Rasor, B. J.; Canter, C.; Jensen, R. O.; Wang, L.; Strutz, J.; Chirania, P.; Tissera, S. D.; Mueller, A. P.; Ruan, Z.; Gao, A.; Tran, L.; Engle, N. L.; Bromley, J. C.; Daniell, J.; Conrado, R.; Tschaplinski, T. J.; Giannone, R. J.; Hettich, R. L.; Karim, A. S.; Simpson, S. D.; Brown, S. D.; Leang, C.; Jewett, M. C.; Köpke, M. Carbon-Negative Production of Acetone and Isopropanol by Gas Fermentation at Industrial Pilot Scale. *Nat. Biotechnol.* **2022**, *40* (3), 335–344. https://doi.org/10.1038/s41587-021-01195-w.

(11) Haas, T.; Krause, R.; Weber, R.; Demler, M.; Schmid, G. Technical Photosynthesis Involving CO2 Electrolysis and Fermentation. *Nat. Catal.* **2018**, *1* (1), 32–39. https://doi.org/10.1038/s41929-017-0005-1.

(12) Portnoy, V. A.; Bezdan, D.; Zengler, K. Adaptive Laboratory Evolution—Harnessing the Power of Biology for Metabolic Engineering. *Curr. Opin. Biotechnol.* **2011**, *22* (4), 590–594. https://doi.org/10.1016/j.copbio.2011.03.007.

(13) Dragosits, M.; Mattanovich, D. Adaptive Laboratory Evolution – Principles and Applications for Biotechnology. *Microb. Cell Factories* **2013**, *12* (1), 64. https://doi.org/10.1186/1475-2859-12-64.

(14) Wannier, T. M.; Kunjapur, A. M.; Rice, D. P.; McDonald, M. J.; Desai, M. M.; Church, G. M. Adaptive Evolution of Genomically Recoded Escherichia Coli. *Proc. Natl. Acad. Sci.* **2018**, *115* (12), 3090–3095. https://doi.org/10.1073/pnas.1715530115.

(15) Kang, S.; Song, Y.; Jin, S.; Shin, J.; Bae, J.; Kim, D. R.; Lee, J.-K.; Kim, S. C.; Cho, S.; Cho, B.-K. Adaptive Laboratory Evolution of Eubacterium Limosum ATCC 8486 on Carbon Monoxide. *Front. Microbiol.* **2020**, *11*, 402. https://doi.org/10.3389/fmicb.2020.00402.

(16) Kim, J.; Cestellos-Blanco, S.; Shen, Y.; Cai, R.; Yang, P. Enhancing Biohybrid CO2 to Multicarbon Reduction via Adapted Whole-Cell Catalysts. *Nano Lett.* **2022**, *22* (13), 5503–5509. https://doi.org/10.1021/acs.nano-lett.2c01576.

(17) Wang, K.; Liu, Y.; Wu, Z.; Wu, Y.; Bi, H.; Liu, Y.; Wang, M.; Chen, B.; Nielsen, J.; Liu, Z.; Tan, T. Investigating Formate Tolerance Mechanisms in Saccharomyces Cerevisiae and Its Application. *Green Carbon* **2023**, *1* (1), 65–74. https://doi.org/10.1016/j.greenca.2023.08.003.

(18) Lechtenberg, T.; Wynands, B.; Müller, M.-F.; Polen, T.; Noack, S.; Wierckx, N. Improving 5-(Hydroxymethyl)Furfural (HMF) Tolerance of Pseudomonas Taiwanensis VLB120 by Automated Adaptive Laboratory Evolution (ALE). *Metab. Eng. Commun.* **2024**, e00235. https://doi.org/10.1016/j.mec.2024.e00235.

(19) Ingelman, H.; Heffernan, J. K.; Harris, A.; Brown, S. D.; Shaikh, K. M.; Saqib, A. Y.; Pinheiro, M. J.; Lima, L. A. de; Martinez, K. R.; Gonzalez-Garcia, R. A.; Hawkins, G.; Daleiden, J.; Tran, L.; Zeleznik, H.; Jensen, R. O.; Reynoso, V.; Schindel, H.; Jänes, J.; Simpson, S. D.; Köpke, M.; Marcellin, E.; Valgepea, K. Autotrophic Adaptive Laboratory Evolution of the Acetogen Clostridium Autoethanogenum Delivers the Gas-Fermenting Strain LAbrini with Superior Growth, Products, and Robustness. *N. Biotechnol.* **2024**, *83*, 1–15. https://doi.org/10.1016/j.nbt.2024.06.002.

(20) Heffernan, J.; Gonzalez, R. A. G.; Mahamkali, V.; McCubbin, T.; Daygon, D.; Liu, L.; Palfreyman, R.; Harris, A.; Koepke, M.; Valgepea, K.; Nielsen, L. K.; Marcellin, E. Adaptive Laboratory Evolution of Clostridium Autoethanogenum to Metabolize CO2 and H2 Enhances Growth Rates in Chemostat and Unravels Proteome and Metabolome Alterations. *Microb. Biotechnol.* **2024**, *17* (4), e14452. https://doi.org/10.1111/1751-7915.14452.

(21) Linley, S.; Reisner, E. Floating Carbon Nitride Composites for Practical Solar Reforming of Pre-Treated Wastes to Hydrogen Gas. *Adv. Sci.* **2023**, *10* (21), 2207314. https://doi.org/10.1002/advs.202207314.

(22) Kim, B. H.; Bellows, P.; Datta, R.; Zeikus, J. G. Control of Carbon and Electron Flow in Clostridium Acetobutylicum Fermentations: Utilization of Carbon Monoxide to Inhibit Hydrogen Production and to Enhance Butanol Yields. *Appl. Environ. Microbiol.* **1984**, *48* (4), 764–770. https://doi.org/10.1128/aem.48.4.764-770.1984.

(23) Allaart, M. T.; Diender, M.; Sousa, D. Z.; Kleerebezem, R. Overflow Metabolism at the Thermodynamic Limit of Life: How Carboxydotrophic Acetogens Mitigate Carbon Monoxide Toxicity. *Microb. Biotechnol.* **2023**, *16* (4), 697–705. https://doi.org/10.1111/1751-7915.14212.

(24) Diender, M.; Stams, A. J. M.; Sousa, D. Z. Production of Medium-Chain Fatty Acids and Higher Alcohols by a Synthetic Co-Culture Grown on Carbon Monoxide or Syngas. *Biotechnol. Biofuels* **2016**, *9* (1), 82. https://doi.org/10.1186/s13068-016-0495-0.

(25) Fackler, N.; Heijstra, B. D.; Rasor, B. J.; Brown, H.; Martin, J.; Ni, Z.; Shebek, K. M.; Rosin, R. R.; Simpson, S. D.; Tyo, K. E.; Giannone, R. J.; Hettich, R. L.; Tschaplinski, T. J.; Leang, C.; Brown, S. D.; Jewett, M. C.; Köpke, M. Stepping on the Gas to a Circular Economy: Accelerating Development of Carbon-Negative Chemical Production from Gas Fermentation. *Annu. Rev. Chem. Biomol. Eng.* **2021**, *12* (1), 1–32. https://doi.org/10.1146/annurev-chembioeng-120120-021122.

(26) Leung, J. J.; Warnan, J.; Ly, K. H.; Heidary, N.; Nam, D. H.; Kuehnel, M. F.; Reisner, E. Solar-Driven Reduction of Aqueous CO2 with a Cobalt Bis(Terpyridine)-Based Photocathode. *Nat. Catal.* **2019**, *2* (4), 354–365. https://doi.org/10.1038/s41929-019-0254-2.

(27) Lam, E.; Reisner, E. A TiO2-Co(Terpyridine)2 Photocatalyst for the Selective Oxidation of Cellulose to Formate Coupled to the Reduction of CO2 to Syngas. *Angew. Chem. Int. Ed.* **2021**, *60* (43), 23306–23312. https://doi.org/10.1002/anie.202108492.